

Iron Catalysis

International Edition: DOI: 10.1002/anie.201612472
German Edition: DOI: 10.1002/ange.201612472

Redox Self-Adaptation of a Nitrene Transfer Catalyst to the Substrate Needs

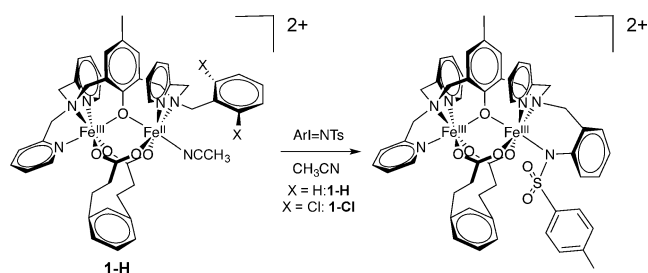
Eric Gouré, Dhurairajan Senthilnathan, Guillaume Coin, Florian Albriex, Frédéric Avenier, Patrick Dubourdeaux, Colette Lebrun, Pascale Maldivi,* and Jean-Marc Latour*

Abstract: The development of iron catalysts for carbon–heteroatom bond formation, which has attracted strong interest in the context of green chemistry and nitrene transfer, has emerged as the most promising way to versatile amine synthetic processes. A diiron system was previously developed that proved efficient in catalytic sulfimidations and aziridinations thanks to an Fe^{III}Fe^{IV} active species. To deal with more demanding benzylic and aliphatic substrates, the catalyst was found to activate itself to a Fe^{III}Fe^{IV}L active species able to catalyze aliphatic amination. Extensive DFT calculations show that this activation event drastically enhances the electron affinity of the active species to match the substrates requirements. Overall this process consists in a redox self-adaptation of the catalyst to the substrate needs.

Nitrene transfer reactions have emerged as the most promising synthetic route to amine derivatives^[1] that are important products or functional intermediates of biological and pharmaceutical relevance.^[2] Several efficient catalytic systems have been reported but most rely on noble metals, especially rhodium.^[3] Replacement of noble metal catalysts by more ecologically and economically friendly first-row transition metal analogues has fueled a considerable amount of work in the past decade. In particular, the search of iron catalysts for many coupling reactions has been intensely developed.^[4] A few active systems were reported for catalytic amination of sulfides and olefins only, and their mechanism is unknown although high valent Fe–nitrene (or imido) active species were postulated.^[5] On the other hand, several high-valent iron–imido (Fe=NR) complexes could be isolated

thanks to Fe ligands of low denticity that promote trigonal or tetrahedral environments to the metal.^[6] However, this strategy was detrimental to the activity. More active five- and six-coordinated iron imido species were reported but could rarely be isolated,^[5a,7] and were at best detected by mass spectrometry techniques.^[7e,8]

We recently reported that the diiron(III,II) complex **1-H** (Scheme 1) is able to mediate the intramolecular nitrene insertion from an iodine (ArI=NTs, Ar=phenyl or 2-tertbutylsulfonylphenyl, Ts=tosyl) into the *ortho* C–H position of the dangling benzyl group of the ligand,^[9] leading



Scheme 1. Top: Intramolecular amination mediated by the diiron(III,II) complex **1-H** [Fe^{III}Fe^{II}(CH₃CN)(mpdp)(L-Bn)]²⁺ leading to the diferric tosylanilate [Fe^{III}Fe^{III}(mpdp)(L-BnNTs)]²⁺ dication (mpdp²⁻ = *m*-phenylenedipropionate). Both compounds were isolated as tetraphenylborate^[11] and perchlorate^[12] salts, respectively.

to a diferric tosylanilate [Fe^{III}Fe^{III}(mpdp)(L-BnNTs)]-(ClO₄)₂. When the *ortho* benzylic positions of the ligand are protected by chlorine atoms, **1-Cl** (Scheme 1) catalyzes efficient intermolecular nitrene transfers to thioanisole (Ph-S-Me) in mild conditions.^[7g] In-depth mechanistic studies^[8] allowed us to show that these catalytic nitrene transfers involve an active diiron(III,IV) tosylimido complex [Fe^{III}Fe^{IV}-(L-BnCl₂)(mpdp)(=NTs)] (Scheme 2A; **3**), which was evidenced by Desorption ElectroSpray Ionization Mass Spectrometry (DESI-MS).^[10] In the present work we demonstrate that, when opposed to more challenging substrates such as ethylbenzene or cyclohexane, the catalysis involves a new formally diiron(III,V) imido amido species [Fe^{III}Fe^V(=NTs)-(NHTs)], **7** (Scheme 2B), which is unprecedented. This new catalytic cycle is thus one oxidation state unit higher than the former one, matching the more difficult oxidation of the substrate. Extensive DFT calculations show indeed that this new active species **7** has a stronger electron affinity than **3** by ca 15 kcal mol⁻¹. These results thus point to a self-adaptation of the catalyst to the oxidizability of the substrate.

[*] Dr. E. Gouré, G. Coin, Dr. F. Avenier, P. Dubourdeaux, Dr. J.-M. Latour
Univ. Grenoble Alpes, CNRS UMR 5249, CEA, LCBM/pmb
38000 Grenoble (France)
E-mail: jean-marc.latour@cea.fr

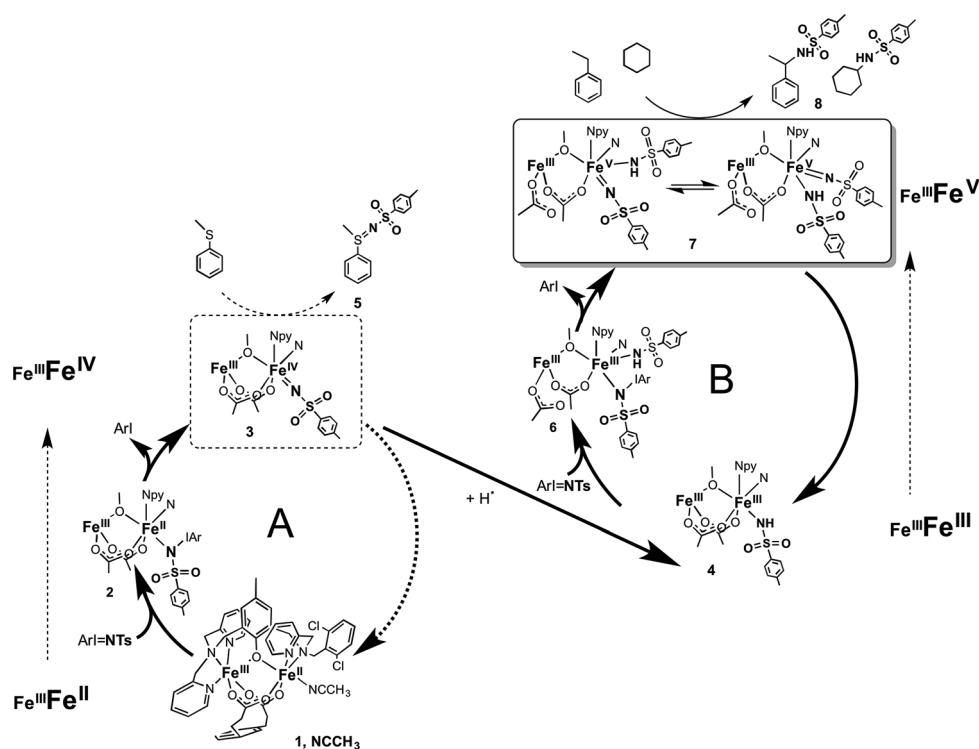
Dr. D. Senthilnathan, C. Lebrun, Dr. P. Maldivi
Univ. Grenoble Alpes, CNRS UMR 5819, CEA, SyMMES
38000 Grenoble (France)
E-mail: pascale.maldivi@cea.fr

Dr. D. Senthilnathan
Center for Computational Chemistry, CRD
PRIST University Vallam, Thanjavur, Tamilnadu (India)

Dr. F. Albriex
CCSM UMR 5246 CNRS—Univ. Claude Bernard
Lyon 1 (France)

Dr. F. Avenier
LCBB, ICMMO (UMR 8182), Univ. Paris Sud, Université Paris Saclay
91405 Orsay (France)

Supporting information for this article can be found under:
<http://dx.doi.org/10.1002/anie.201612472>.



Scheme 2. Species occurring during nitrene transfers mediated by 1-Cl as detected by DESI-MS experiments. The label “-Cl” was omitted for simplicity and because corresponding species are formed from 1-H. Species **7** exists under two tautomeric forms evidenced by ESI-MS experiments and DFT calculations, see Figure 1 and the Supporting Information, Figure S13.

The catalytic ability of the 1-Cl/PhI=NTs system was assayed in the amination of substituted ethylbenzenes and THF. In a typical reaction 1-Cl, PhI=NTs and the substrate in 0.05:1:100 ratio were reacted for 5 h in dichloromethane at room temperature. The tosylamines $C_6H_5CH(NHTs)CH_3$ and $(C_4H_7O)(NHTs)$ were isolated in circa 50% yields (vs. PhI=NTs; see the Supporting Information, Table S1). The UV/Vis spectra recorded during catalytic amination of ethylbenzene (Supporting Information, Figure S1a) are dominated by an intense absorption at 482 nm, which is associated to the diferric amido derivative 4-Cl (Scheme 2).^[7g,8] By contrast, corresponding spectra recorded during catalytic amination of thioanisole exhibit an absorption at 580 nm (Supporting Information, Figure S1b) indicating that a mixed-valent $Fe^{III}Fe^{II}$ species 1-Cl/2-Cl is the resting species during catalysis. These observations indicate that the amination of ethylbenzene or cyclohexane does not follow the catalytic cycle A (Scheme 2). 4-Cl is formed by H^+ abstraction by 3-Cl from an external H^+ donor (such as dihydroanthracene or diphenylhydrazine, H_2 -DPH) or from a benzylic position of the ligands.^[7g,8] It is not intrinsically capable of nitrene transfer, and therefore a second catalytic cycle must exist involving its activation by PhI=NTs.

Apart from the known patterns at 464, 494, 549, and 710.5, (corresponding, respectively to 1-Cl²⁺, the protonated iodine adduct $[ArI=NTs, H]^+$, the mixture 3-Cl²⁺/4-Cl²⁺, and 2-Cl²⁺ (Scheme 2 A),^[7g] the DESI-MS spectrum recorded immediately after mixing 1-Cl and ArI=NTs at room temperature in acetonitrile (Supporting Information, Figure S2) revealed

unassigned patterns at 634.5 and 795.5. The mass value, the isotopic profile and the shift of 0.5 mass unit induced by the use of $ArI=^{15}NTs$ concur to show (Supporting Information, Figure S3) that the pattern at m/z 794–800 is due to 6-Cl²⁺, the iodine adduct of 4-Cl²⁺, $[Fe^{III}Fe^{III}(L-BnCl_2)(mpdp)(NHTs)]^{2+}$ ($ArI=NTs$)²⁺. A similar analysis of the pattern at m/z 632–638 (Supporting Information, Figure S2, inset and Figure S4) associates it to species 7-Cl²⁺ best formulated as the diiron(III,V) imido amido species $[Fe^{III}Fe^V(L-BnCl_2)(mpdp)(=NTs)(-NHTs)]^{2+}$, the expected species resulting from the 2-electron-oxidative addition of tosyl nitrene to 4-Cl.

To further characterize **7** and prove its ability to transfer the NTs group to various substrates, we first generated quantitatively 4-Cl or 4-H and investigated their reactivity in

benchmark reactions, respectively the intermolecular nitrene transfer to thioanisole and in the intramolecular reaction with the pendant benzyl group of the ligand. Moreover, to trace the origin of the transferred NTs group, we used different labelings of the imido and amido groups. In a first step, 4-Cl (4-H) was generated by reaction of 1-Cl (1-H) with one equiv ArI=NTs in the presence of one equiv DHA. In the intermolecular transfer experiment, 4-Cl was treated by 10 equivalents PhSMe and then one equiv of $ArI=^{15}NTs$, and the produced sulfolimine PhS(NTs)Me was isolated and analyzed by ESI-MS (Supporting Information, Figure S5). The isotopic distribution in the 294–299 range can be reproduced taking into account a 2:98 mixture of $^{14}N/^{15}N$ isotopomers. This experiment shows that the NTs group transferred to the substrate originates essentially from the second introduced iodine. In the intramolecular transfer experiment, 4-H was treated by one equiv of $ArI=^{15}NTs$ and the product of the reaction was analyzed by ESI-MS. Examination of the pattern at 513–517 (Supporting Information, Figure S6) corresponding to the species $[Fe^{III}Fe^{III}(mpdp)(L-BnNTs)]^{2+}$ (Scheme 1) revealed the insertion of either ^{14}NTs or ^{15}NTs groups in comparable amounts (42 vs. 58%, respectively). These apparently conflicting results between inter- and intramolecular NTs transfers can be easily reconciled by considering the widely different rates of the two reactions and the occurrence of a tautomeric equilibrium within **7** (Scheme 2).

Indeed, whereas an imido group can be transferred to substrates, an amido group cannot. Hence, to be transferred

the amido group in **7** must have been transformed into an imido group, and the simplest way to achieve this transformation is a tautomeric equilibrium between the imido and amido groups as shown for oxo/hydroxo derivatives.^[13] With such a process going on, the eventual labeling of the product in the two reactions is dependent on the kinetic competition between the proton exchange and the nitrene transfer. Indeed, as shown by UV/Vis experiments the intramolecular nitrene transfer to the benzyl group occurs on the minute time scale, slow enough to allow for the tautomeric equilibrium to be fully established explaining that both ¹⁴NTs and ¹⁵NTs groups are transferred equally. By contrast, the nitrene transfer to thioanisole occurs in the millisecond time scale, faster than the proton exchange, explaining that only the labeled nitrene ¹⁵NTs group is transferred since the tautomeric equilibrium has not yet progressed.

To substantiate this mechanistic scheme, we reasoned that slowing down the intermolecular transfer to thioether substrates should allow for increased transfer of the ¹⁴NTs group. This can be achieved by using less reactive sulfides and/or performing the reaction at lower temperature. Indeed both factors lead to an increased content of the ¹⁴NTs isotopomer attesting the progress of the tautomeric equilibrium (Supporting Information, Table S2 and Figures S7, S8). We obtained the ultimate confirmation for the latter by evidencing a kinetic influence of H/D substitution within **4-Cl** [^{Fe^{III}Fe^{III}(-NHTs)]. Reacting D-labeled **4-Cl** [^{Fe^{III}Fe^{III}(-NDTs)] with ArI=¹⁵NTs in the presence of PhSPh(NO₂) at -30°C as before led to a diminished ¹⁴NTs transfer, as expected (Supporting Information, Figure S8). This weak effect is significant and reproducible and consistent with very recent observations made on oxo/hydroxo exchange.^[14] All the above observations thus establish that aliphatic aminations involve a second catalytic cycle (Scheme 2 B), of which the active species **7** is generated by activation of **4** and exists as an equilibrium of two tautomers.}}

In the absence of any possible spectroscopic characterization of **7** due to its transient nature, we relied on DFT theoretical calculations to get insights into its molecular and electronic structures. We followed a similar protocol as in our previous study of **3** and **4**,^[8] exploring several initial structures and spin state configurations (see the Supporting Information for more details). The most reasonable model involves binding of the two N(H)Ts groups on the same Fe ion (Fe_B, Figure 1), concurring with the tautomeric equilibrium.

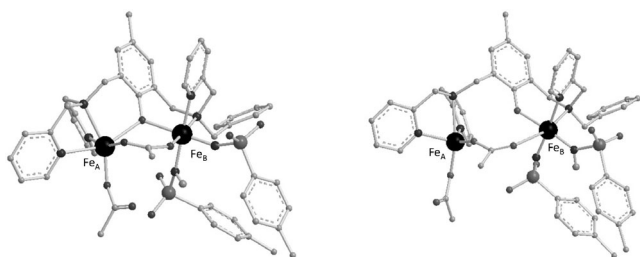


Figure 1. Optimized geometries (top) of the two lowest energy configurations for the two models of **7** Nt-NHc (left) and NHt-Nc (right). H atoms are not represented except the H in the NHTs ligand (in ball-and-stick mode).

Examination of energy differences at various computational levels pointed to only two low energy geometries, one with NTs *trans* vs. the phenoxide group (denoted OPh below) and NHTs *cis* (denoted below Nt_NHc) and one with NHTs *trans* and NTs *cis* (denoted below NHt_Nc). The energy differences between these two isomers are within a 0.3 eV range, depending on the theoretical level (Supporting Information, Tables S6, S7). This value can be considered as a reasonable uncertainty at this level of computation, thus both isomers must be considered as isoenergetic. Their geometries are represented on Figure 1.

As expected Fe_B-N distances (from NTs and NHTs) vary slightly for the different electronic configurations but cluster around a representative value (Supporting Information, Tables S4, S5). For both isomers the Fe_B-N_{Ts} distance is about 1.77 Å, similar to the values already obtained for the mixed-valent species **3** (1.8 Å) and to the distance found by EXAFS by Klinker et al.^[7c] for the [(N4Py)Fe^{IV}(NTs)] complex (1.73 Å). The Fe_B-N_{NHTs} distances are longer (1.89 to 1.97 Å), and perfectly consistent with the ones reported for Fe^{III}-NHTs complexes^[15] and that found in the binuclear complex **4** (1.94 to 1.97 Å).^[8]

Examination of the spin densities of both Fe ions and NTs, NHTs, and OPh ligands (Table 1; Supporting Information, Tables S6, S7) reveal remarkable features. First, the spin densities for Fe_A are always between 4 and 4.13, typical of

Table 1: Spin densities of Fe_B, NTs, NHTs, and OPh groups from SP B3LYP in the gas phase for NHt_Nc and Nt_NHc isomers, in the low energy spin configuration identified through total spin projection Sz = 5.^[a]

	Fe _A	Fe _B	NTs	NHTs	OPh	Electronic configuration
NHt_Nc	4.08	2.72	1.09	0.24	0.85	Fe ^{III} , Fe ^{IV} -OPh, NTs
Nt_NHc	4.13	3.23	1.05	0.59	-0.01	Fe ^{III} , Fe ^{IV} -OPh, *NTs

[a] Other hybrid functionals (B3LYP*, PBE0, M06, TPSSH) or solvent phase calculations give very similar results within a 0.2 eV energy range (see the Supporting Information).

a high spin Fe^{III} ion, and similar to those found in complexes **3** and **4**, showing that Fe_A is not affected by the redox change from **4** to **7**. Second, by contrast, the Fe_B ion exhibits much lower values close or lower than 3. Third, in all cases, a full radical character is present on OPh and/or NTs ligands. Thorough examinations of the Kohn-Sham orbitals combined with these spin density values lead to a consistent picture of the electronic structures of both tautomers. For the NHt_Nc isomer, the LUMO is localized on an OPh π orbital supporting the oxidation of the phenoxide (Supporting Information, Figure S9, S10). In contrast, for Nt_NHc isomer the LUMO is localized on an imido π orbital (Supporting Information, Figures S11, S12). Finally, in both cases, Fe_B is a high spin d⁴ Fe^{IV} ion, although its spin density values are highly depleted compared to an expected value close to **4**, owing to strong donation effects. Hence a clear picture emerges for the activated species **7**. Its generation by the two-electron oxidation of **4** occurs through a one-electron oxidation of Fe_B to give an Fe^{IV} ion and a one-electron oxidation of one ligand. Owing to the strong *trans* effect of the

imido ligand, either the phenoxide (NHt_Nc tautomer) or the NTs group (Nt_NHc tautomer) is oxidized, leading, respectively, to the formal electronic configurations $\text{Fe}^{\text{III}}\text{Fe}^{\text{IV}}\text{-OPh}$ and $\text{Fe}^{\text{III}}\text{Fe}^{\text{IV}}\text{-NTs}$.

In line with the fast tautomeric equilibrium, our optimized geometries show a short distance (2.45–2.50 Å) between H from the amido group and N from the imido group within both tautomers (Figure 1; Supporting Information, Figure S13). Using this distance as a reaction coordinate, we carried out a computational modeling of the possible mechanism for this exchange. It allowed us to characterize a transition state with an activation free energy of 23.3 kcal mol⁻¹ (see the Supporting Information for details). We compared this barrier to the only known computed value of activation energy of a Fe-based NTs transfer to dimethylsulfide provided by de Visser et al. (ca. 18 kcal mol⁻¹ at the same computational level).^[16] This comparison shows that both activation energies (tautomerism and NTs transfer to organic sulfide) are close, although the NTs transfer activation energy is slightly lower than that of the tautomeric equilibrium. These computations are in full agreement with experimental observations that both reactions have competitive rates. To sum up these computational investigations on **7**, the two-electron oxidative addition of NTs to **4** leading to **7** corresponds to a change from a $\text{Fe}^{\text{III}}\text{Fe}^{\text{III}}$ binuclear core to a $\text{Fe}^{\text{III}}\text{Fe}^{\text{IV}}\text{-L}\cdot$ (L being one of the ligand on Fe_{B}), and not to any possible $\text{Fe}^{\text{IV}}\text{Fe}^{\text{IV}}$ or $\text{Fe}^{\text{III}}\text{Fe}^{\text{V}}$ valence localizations. Moreover, the two resulting tautomers are very close in energy, and can easily exchange the amide proton competitively with NTs intermolecular transfer, consistently with the experimentally observed equilibria.

We have shown that the present diiron system is able to catalyze very efficient nitrene transfers to a variety of substrates ranging from thioethers and aziridines^[7b,9] to more demanding aliphatic substrates. This compares favorably with the most active non-heme iron systems reported so far.^[5,7c] This strong activity is based on its peculiar ability to be activated twice for nitrene transfer. Indeed, reaction of **1-Cl** with $\text{PhI}=\text{NTs}$ involves two independent but connected cycles based on the same sequence of reactions: binding of the iodine to the catalyst (**1**→**2** and **4**→**6**), intramolecular two-electron rearrangement with PhI elimination generating an active high-valent intermediate (**2**→**3** and **6**→**7**) and nitrene transfer to the substrate regenerating the catalyst (**3**→**1** and **7**→**4**). The two cycles are connected by deactivation of **3**, a $\text{Fe}^{\text{III}}\text{Fe}^{\text{IV}}$ active state, through $\text{H}\cdot$ abstraction to the corresponding amido derivative **4** that is reactivated in cycle B, which is similar to A but one oxidation state higher with an $\text{Fe}^{\text{III}}\text{Fe}^{\text{IV}}\text{-L}\cdot$ species (**7**) as a new active intermediate.

Our DFT investigations of the electronic structure of **7** are fully consistent with the electrophilic nature of the catalytic active species as experimentally evidenced. The Kohn–Sham orbital diagrams (Supporting Information, Figures S9–S12) exhibit a LUMO exclusively localized on one of the ligands OPh (for NHt_Nc) or NTs (for Nt_NHc) with quite low HOMO–LUMO gaps between 0.7 and 1.3 eV. These remarkable electronic properties point to a high electrophilicity, which is expected to yield a strong electron affinity (EA) and a high H-atom abstracting ability, measured by the magnitude

of BDE (NH). These values have been computed for **7** and **3** and compared to those of the best documented related system $[(\text{N4Py})\text{Fe}^{\text{IV}}(\text{NTs})]$,^[7c,16,17] (see the Supporting Information and Table S10). A notable increase in EAs is observed for **7** (142.7 kcal mol⁻¹) compared to **3** (127.5 kcal mol⁻¹) and to $[(\text{N4Py})\text{Fe}^{\text{IV}}(\text{NTs})]$ (129.6 kcal mol⁻¹). This increase is consistent with the higher oxidation state of **7**. By contrast, the magnitude of BDE (NH) is found similar for **3** (99.7 kcal mol⁻¹) and **7** (95.9 kcal mol⁻¹) and higher than $[(\text{N4Py})\text{Fe}^{\text{IV}}(\text{NTs})]$ (89.0 kcal mol⁻¹). This supports that EA is the major factor contributing to the higher activity of the present system.

Along with this high activity, the most salient feature is that the active species involved is dependent on the oxidizability of the substrate: an easy substrate is aminated through cycle A, whereas a more demanding one triggers activation of cycle B relying on a more electrophilic active species. This process is akin to a redox induced fit, which is unprecedented to the best of our knowledge. The fact that a single Fe ion is involved in the redox changes opens the way to mononuclear catalysts operating along the same line.

Acknowledgements

J.M.L. and P.M. thank the French National Agency for Research (ANR) “programme Labex” (ARCANE project no. ANR-11-LABX-003) for partial funding. This work was performed using HPC resources from GENCI-CINES (Grant 2015-c2016087648).

Conflict of interest

The authors declare no conflict of interest.

Keywords: amination · homogeneous catalysis · iron · nitrene · tautomerism

- [1] a) H. M. L. Davies, J. R. Manning, *Nature* **2008**, *451*, 417–424; b) G. Dequierez, V. Pons, P. Dauban, *Angew. Chem. Int. Ed.* **2012**, *51*, 7384–7395; *Angew. Chem.* **2012**, *124*, 7498–7510; c) P. Starkov, T. F. Jamison, I. Marek, *Chem. Eur. J.* **2015**, *21*, 5278–5300.
- [2] S. Roughley, A. M. Jordan, *J. Med. Chem.* **2011**, *54*, 3451–3479.
- [3] J. Roizen, M. Harvey, J. Du Bois, *Acc. Chem. Res.* **2012**, *45*, 911–922.
- [4] a) A. Correa, O. Garcia Mancheno, C. Bolm, *Chem. Soc. Rev.* **2008**, *37*, 1108–1117; b) B. Su, Z.-C. Cao, Z.-J. Shi, *Acc. Chem. Res.* **2015**, *48*, 886–896.
- [5] a) J. Wang, M. Frings, C. Bolm, *Angew. Chem. Int. Ed.* **2013**, *52*, 8661–8665; *Angew. Chem.* **2013**, *125*, 8823–8827; b) A. Fingerhut, O. V. Serdyuk, S. B. Tsogoeva, *Green Chem.* **2015**, *17*, 2042–2058.
- [6] a) P. L. Holland, *Acc. Chem. Res.* **2008**, *41*, 905–914; b) C. T. Saouma, J. C. Peters, *Coord. Chem. Rev.* **2011**, *255*, 920–937; c) E. R. King, E. T. Hennessy, T. A. Betley, *J. Am. Chem. Soc.* **2011**, *133*, 4917–4923.

- [7] a) J. P. Mahy, P. Battioni, D. Mansuy, *J. Am. Chem. Soc.* **1986**, *108*, 1079–1080; b) M. P. Jensen, M. P. Mehn, L. Que, Jr., *Angew. Chem. Int. Ed.* **2003**, *42*, 4357–4360; *Angew. Chem.* **2003**, *115*, 4493–4496; c) E. J. Klinker, T. A. Jackson, M. P. Jensen, A. Stubna, G. Juhasz, E. L. Bominaar, E. Münck, L. Que, Jr., *Angew. Chem. Int. Ed.* **2006**, *45*, 7394–7397; *Angew. Chem.* **2006**, *118*, 7554–7557; d) P. Leeladee, G. N. L. Jameson, M. A. Siegler, D. Kumar, S. P. de Visser, D. P. Goldberg, *Inorg. Chem.* **2013**, *52*, 4668–4682; e) Y. Liu, X. Guan, E. L.-M. Wong, P. Liu, J.-S. Huang, C.-M. Che, *J. Am. Chem. Soc.* **2013**, *135*, 7194–7204; f) S. Cramer, R. Hernandez Sanchez, D. Brakhage, D. Jenkins, *Chem. Commun.* **2014**, *50*, 13967–13970; g) F. Avenier, J.-M. Latour, *Chem. Commun.* **2004**, 1544–1545.
- [8] E. Gouré, F. Avenier, P. Dubourdeaux, O. Sénèque, F. Albrieux, C. Lebrun, M. Clémancey, P. Maldivi, J.-M. Latour, *Angew. Chem. Int. Ed.* **2014**, *53*, 1580–1584; *Angew. Chem.* **2014**, *126*, 1606–1610.
- [9] F. Avenier, E. Gouré, P. Dubourdeaux, O. Sénèque, J.-L. Oddou, J. Pécaut, S. Chardon-Noblat, A. Deronzier, J.-M. Latour, *Angew. Chem. Int. Ed.* **2008**, *47*, 715–717; *Angew. Chem.* **2008**, *120*, 727–729.
- [10] a) Z. Takats, J. M. Wiseman, B. Gologan, R. G. Cooks, *Science* **2004**, *306*, 471–473; b) R. H. Perry, T. J. Cahill III, J. L. Roizen, J. Du Bois, R. N. Zare, *Proc. Natl. Acad. Sci. USA* **2012**, *109*, 18295–18299.
- [11] W. Kanda, W. Moneta, M. Bardet, E. Bernard, N. Debaecker, J. Laugier, A. Bousseksou, S. Chardon-Noblat, J.-M. Latour, *Angew. Chem. Int. Ed. Engl.* **1995**, *34*, 588–590; *Angew. Chem.* **1995**, *107*, 625–628.
- [12] S. Chardon-Noblat, O. Horner, B. Chabut, F. Avenier, N. Debaecker, P. Jones, J. Pécaut, L. Dubois, C. Jeandey, J.-L. Oddou, et al., *Inorg. Chem.* **2004**, *43*, 1638–1648.
- [13] J. Bernadou, B. Meunier, *Chem. Commun.* **1998**, 2167–2173.
- [14] M. Puri, A. Company, G. Sabenya, M. Costas, L. Que, *Inorg. Chem.* **2016**, *55*, 5818–5827.
- [15] a) N. A. Eckert, S. Vaddadi, S. Stoian, R. J. Lachicotte, T. R. Cundari, P. L. Holland, *Angew. Chem. Int. Ed.* **2006**, *45*, 6868–6871; *Angew. Chem.* **2006**, *118*, 7022–7025; b) M. K. Zart, D. Powell, A. S. Borovik, *Inorg. Chim. Acta* **2007**, *360*, 2397–2402; c) H. S. Soo, M. T. Sougrati, F. Grandjean, G. J. Long, C. J. Chang, *Inorg. Chim. Acta* **2011**, *369*, 82–91.
- [16] a) S. Kumar, A. S. Faponle, P. Barman, A. K. Vardhaman, C. V. Sastri, D. Kumar, S. P. de Visser, *J. Am. Chem. Soc.* **2014**, *136*, 17102–17115; b) A. K. Vardhaman, P. Barman, S. Kumar, C. V. Sastri, D. Kumar, S. P. de Visser, *Angew. Chem. Int. Ed.* **2013**, *52*, 12288–12292; *Angew. Chem.* **2013**, *125*, 12514–12518.
- [17] A. K. Vardhaman, Y.-M. Lee, J. Jung, K. Ohkubo, W. Nam, S. Fukuzumi, *Angew. Chem. Int. Ed.* **2016**, *55*, 3709–3713; *Angew. Chem.* **2016**, *128*, 3773–3777.

Manuscript received: December 23, 2016

Final Article published: ■ ■ ■ ■, ■ ■ ■ ■ ■

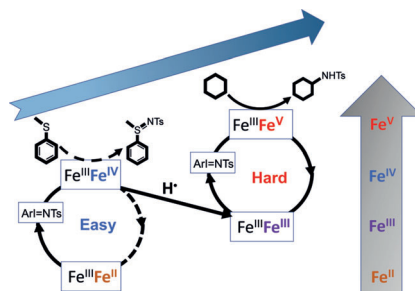
Communications



Iron Catalysis

E. Gouré, D. Senthilnathan, G. Coin,
F. Albrieux, F. Avenier, P. Dubourdeaux,
C. Lebrun, P. Maldivi,*
J.-M. Latour*     

Redox Self-Adaptation of a Nitrene
Transfer Catalyst to the Substrate Needs



Self-adaptive catalyst: An efficient diiron catalyst mediates nitrene transfer to sulfides through an Fe^{IV} active state but self-activates to Fe^V when facing aliphatic substrates that are harder to oxidize.